AIAA JOURNAL
Vol. 47, No. 3, March 2009

Aerospace Letters

AEROSPACE LETTERS are brief communications (approximately 2000 words) that describe new and potentially important ideas or results, including critical analytical or experimental observations that justify rapid publication. They are stringently prescreened, and only a few are selected for rapid review by an Editor. They are published as soon as possible electronically and then appear in the print version of the journal.

Self-Induced Roll Oscillations of Nonslender Wings

Nicholas T. Gresham,* Zhijin Wang,† and Ismet Gursul‡
University of Bath, Bath, England BA2 7AY, United Kingdom

DOI: 10.2514/1.42511

Introduction

SELF-INDUCED roll oscillation of *slender* delta wings, referred to as wing rock, is a well-known fluid–structure interaction and is driven by the leading-edge vortices [1,2]. Similar roll oscillations were observed, as sketched in Fig. 1a, for very-low-aspect-ratio rectangular wings, as the tip (or side-edge) vortices drive the motion [3,4]. Previous experimental evidence has suggested that these limit-cycle roll oscillations are unique to slender delta wings and rectangular wings, for which the vortices are relatively close to each other. In this Letter, we show that such roll oscillations are possible for wings with much larger aspect ratios, as sketched in Fig. 1b, even though vortex interactions are thought to be unlikely.

Previous studies showed that slender delta wing rock is possible for sweep angles larger than 75 deg (aspect ratio $Æ = 0.54$). Similarly, very-low-aspect-ratio rectangular wings exhibit wing rock for $Æ < 0.5$ due to the proximity of the tip vortices. In this Letter, we show that *nonslender* wings (with aspect ratios up to $Æ = 4$) of various planform shapes shown in Fig. 1b exhibit wing rock despite the fact that the tip vortices are not as close to each other. Our measurements indicate that the motion is driven by the vortex dynamics and vortex–wing interaction, because there is no interaction between the vortices. This surprising discovery has important implications for small aircraft flying at low Reynolds numbers [5,6].

Experimental Setup

The experiments were carried out in the University of Bath's closed-loop wind tunnel with a test section of 2.1×1.5 m. Figure 1b shows the flat-plate wing planforms tested, which included Zimmerman [taken from [7], a common micro air vehicle (MAV) planform] with chord length ($c = 0.213$ m, span $b = 0.335$ m, and $Æ = 1.93$), elliptical ($c = 0.1675$ m, $b = 0.335$ m, and $Æ = 2.55$), and rectangular wings ($c = 0.1675$ m, $b = 0.335$ m, and $Æ = 2$ and $c = 0.1675$ m, $b = 0.67$ m, and $Æ = 4$). The Reynolds number based on the root chord length varied in the range of $Re = 114{,}000$ to 435,000. The wings were made of aluminum and had a thickness of 3 mm. All edges on all wings were round (semicircular). In addition, a second $Æ = 2$ rectangular-wing model with sharp edges was also tested. All models used the same sting support, which attached to the wings on the pressure surface, thus leaving the suction surface clean. The model and sting were mounted upon a shaft that was free to rotate in low-friction bearings and attached to a potentiometer, which fed a signal via an A/D converter to a PC at a rate of 250 Hz for 90 s over a range of angles of attack. From these data, the standard deviation of the roll angle of the oscillations was calculated and the Strouhal number of the oscillations was obtained using a fast Fourier transform.

A particle image velocimetry (PIV) system with dual 120 mJ Nd:YAG lasers was used to capture the crossflow velocity field for the rectangular wing with $Æ = 2$ and round edges at the midchord streamwise station ($x/c = 0.5$). Three separate tests were needed to cover the extent of the wing span. Only every third vector is shown in the PIV results for clarity. The results shown incorporate both dynamic cases (in which the wing was set to trigger at specific roll angles during the roll oscillations) and a static case (with the wing clamped at the desired roll angle). To measure the strength of the side-edge vortices from the PIV data, circulation was calculated using a line integral around the region of interest and normalized using the freestream velocity and chord length.

Results and Discussion

A typical free-to-roll time history of a wing undergoing self-excited roll oscillations is shown in Fig. 2. The wing in this case is the rectangular wing with $Æ = 2$ and round edges. The oscillations can be seen to be periodic and of large amplitude with a slightly nonzero mean roll angle in this case, which we will come back to in the discussion of the PIV data. The wing is at an angle of attack of $\alpha = 15$ deg in the poststall regime (this was confirmed with tuft visualization, but not shown here). The data presented here show the first documented case of a wing of such an aspect ratio exhibiting these oscillations. Levin and Katz [3] reported that self-induced roll oscillations of rectangular wings were possible when the aspect ratio was less than 0.5. No free-to-roll experiments on wings with larger aspect ratios have been reported in the literature; hence, the discovery of oscillations for this wing and for $Æ = 4$ is interesting and unexpected.

Results for all wings are summarized in Fig. 3, with Fig. 3a showing how the standard deviation of the roll angle increased with increasing angle of attack in the poststall regime. The results for the

Received 2 December 2008; accepted for publication 10 December 2008; published online 21 January 2009.

*Postgraduate Student, Department of Mechanical Engineering. Member AIAA.
†Research Councils United Kingdom Academic Fellow, Department of Mechanical Engineering.
‡Professor, Department of Mechanical Engineering. Associate Fellow AIAA.

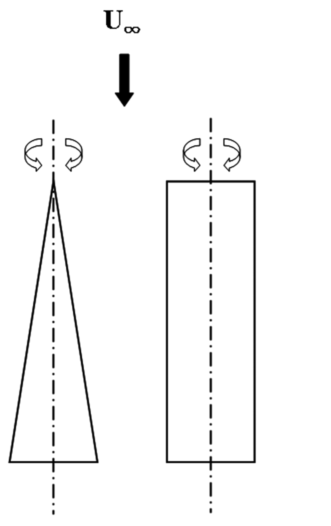

a)

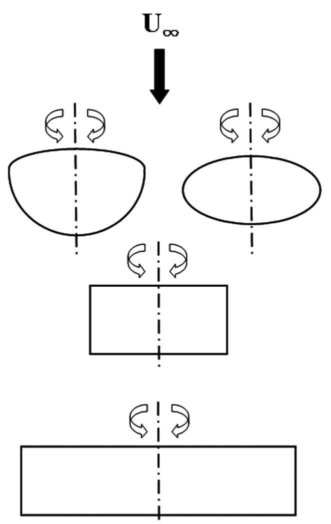

b)

Fig. 1 Schematic of a) roll oscillations of a slender delta wing (left) and a low-aspect-ratio rectangular wing (right) and b) wings tested, comprising Zimmerman (top left), elliptical (top right), rectangular wing of Æ = 2 (center), and rectangular wing of Æ = 4 (bottom).

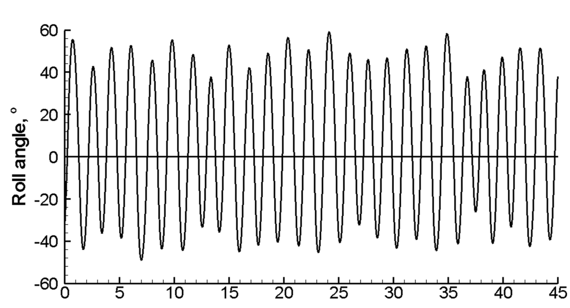

Fig. 2 Time history of roll angle at $\alpha = 15$ deg and $Re = 1.14 \times 10^5$ for a rectangular wing with Æ = 2 and round edges.

rectangular wing with Æ $= 2$ and round edges show that the oscillations become larger with increasing Reynolds number. The rectangular wings with Æ $= 2$ and different edge geometry exhibited similar standard deviations once the oscillations became large. The rectangular wing with Æ $= 4$ exhibited the largest roll oscillations out of all the wings. The other two wings (Zimmerman and elliptical) also demonstrated previously unseen roll oscillations,

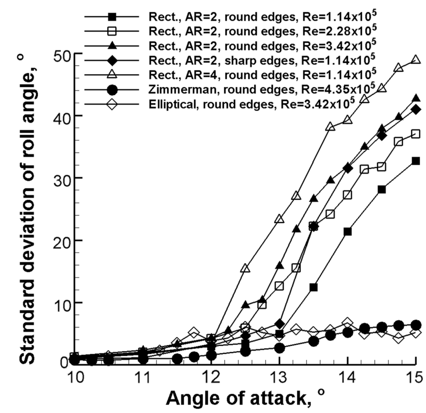

a)

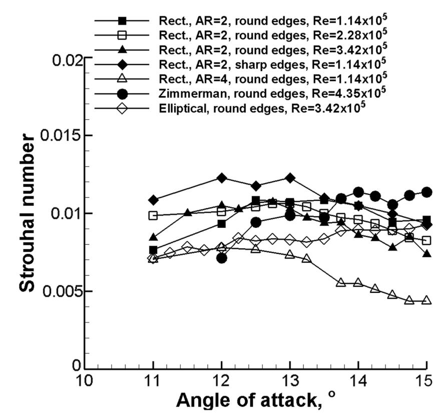

b)

Fig. 3 Variation of a) standard deviation with angle of attack and b) Strouhal number with angle of attack.

shown by the increasing standard deviation with angle of attack, though the oscillations were much smaller in amplitude than those for the rectangular wings.

Figure 3b shows the variation of Strouhal number, fc/U_∞, where U_∞ is the freestream velocity and f is the frequency. Note that all the Strouhal numbers are low, of the order of 10^{-2}, similar to those expected for MAVs encountering typical atmospheric gusts. It is seen that the frequency of oscillation decreases slightly as angle of attack is increased for all rectangular wings once the amplitude starts to increase (shown by the liftoff in the slopes in Fig. 3a), whereas the Strouhal number is seen to increase for the Zimmerman and elliptical wings. The effects of Reynolds number and sharp edges for the rectangular wings with Æ $= 2$ are not significant. The rectangular wing with Æ $= 4$ shows the lowest Strouhal number of oscillations, presumably because of its higher moment of inertia about the roll axis.

To investigate the aforementioned oscillations of the rectangular wings further, PIV measurements were performed for the Æ $= 2$ wing. Figure 4a shows the static case (at a slightly nonzero mean roll angle of $\phi = 3$ deg, as mentioned earlier), and the salient feature to note is the symmetry of the flow structure, with each side-edge vortex being of similar size. The nondimensional circulation $\Gamma/U_\infty c$ of the left-hand vortex is -0.20, whereas that of the right-hand vortex is 0.23, the difference being due to the slightly nonzero mean roll angle. This symmetry is lost in the dynamic case of Fig. 4b at the same roll angle. When the wing rolls in the clockwise direction (top of Fig. 4b), the tip vortex is stronger on the left-hand side ($\Gamma/U_\infty c = -0.23$), which is larger than in the static case and also closer to the wing surface than the one on the right-hand side of the wing ($\Gamma/U_\infty c = 0.19$, smaller than in the static case). When the wing reaches the maximum roll angle ($\phi = 36$ deg), the right-hand vortex is strong ($\Gamma/U_\infty c = 0.32$) and has been seen to move inboard, whereas the left-hand vortex is small and weak ($\Gamma/U_\infty c = -0.08$). The stronger vortex on the right-hand side provides the restoring moment. As the wing rolls in the opposite (anticlockwise) direction,

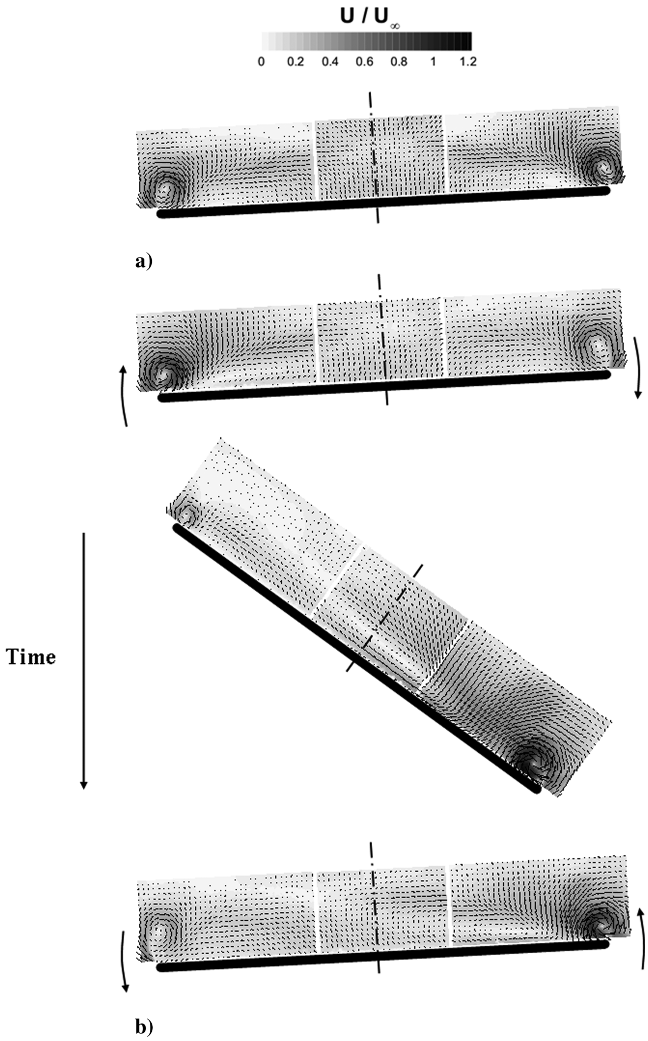

Fig. 4 Crossflow velocity field for a) stationary wing at mean roll angle and b) rolling wing at mean (top), maximum (middle), and mean (bottom) roll angles, at $\alpha = 15$ deg, $x/c = 0.5$, and $Re = 1.14 \times 10^5$ for a rectangular wing with $AR = 2$ and round edges.

at the mean roll angle of $\phi = 3$ deg (bottom of Fig. 4b), there is an asymmetry in the vortical flow, with the right-hand vortex in this case providing the driving motion. The nondimensional circulations are −0.16 for the left-hand vortex (smaller than in the static case) and 0.24 for the right-hand vortex (which is slightly larger than in the static case). The different flow structures that are possible at the same roll angle demonstrate the hysteresis and time-lag effects that are present in the flow. These observations are similar to the hysteresis and time lag of the position of the vortices over slender delta wings during wing-rock motion [1,2].

Conclusions

Self-induced roll oscillations have been found for rectangular wings with much higher aspect ratios than previously reported. Tip (side-edge) vortices are not close to each other for these wings, unlike those for very slender wings. The limit-cycle roll oscillations are observed despite the absence of any interaction between the vortices. Velocity measurements revealed the variations in the position and strength of the vortices during the rolling motion. There is a time lag in the strength of the vortices, which drives the motion for the rolling wing. This effect is best demonstrated at the mean roll angle, resulting in an asymmetric crossflow and a net rolling moment in the direction of the rolling motion. Self-induced roll oscillations, though smaller in amplitude, were also found for Zimmerman and elliptical planforms. These findings are highly relevant to micro air vehicles and unmanned air vehicles.

Acknowledgments

This work is sponsored by the U.S. Air Force Office of Scientific Research, Air Force Material Command, U.S. Air Force, under grant number FA8655-06-1-3058, and by the Engineering and Physical Sciences Research Council Academic Fellowship in Unmanned Air Vehicles.

References

[1] Katz, J., "Wing/Vortex Interactions and Wing Rock," *Progress in Aerospace Sciences*, Vol. 35, No. 7, 1999, pp. 727–750. doi:10.1016/S0376-0421(99)00004-4
[2] Arena, A. S., and Nelson, R. C., "Experimental Investigation on Limit Cycle Wing Rock of Slender Wings," *Journal of Aircraft*, Vol. 31, No. 5, 1994, pp. 1148–1155. doi:10.2514/3.46625
[3] Levin, D., and Katz, J., "Self-Induced Roll Oscillations of Low-Aspect-Ratio Rectangular Wings," *Journal of Aircraft*, Vol. 29, No. 4, 1992, pp. 698–702. doi:10.2514/3.46222
[4] Williams, D. L., and Nelson, R. C., "Fluid-Dynamic Mechanisms Leading to the Self-Induced Oscillations of LARR Wings," 35th Aerospace Sciences Meeting and Exhibit, AIAA Paper 97-0830, Reno, NV, Jan. 1997.
[5] Mueller, T. J., and DeLaurier, J. D., "Aerodynamics of Small Vehicles," *Annual Review of Fluid Mechanics*, Vol. 35, Jan. 2003, pp. 89–111. doi:10.1146/annurev.fluid.35.101101.161102
[6] Shyy, W., Berg, M., and Ljungqvist, D., "Flapping and Flexible Wings for Biological and Micro Air Vehicles," *Progress in Aerospace Sciences*, Vol. 35, No. 5, 1999, pp. 455–505. doi:10.1016/S0376-0421(98)00016-5
[7] Zimmerman, C. H., "Aerodynamic Characteristics of Several Airfoils of Low Aspect Ratio," NACA TN-539, Aug. 1935.

E. Oran
Editor-in-Chief